


Fullerenes | Hot Paper |

 Unusual C_{2h} -Symmetric *trans*-1-(Bis-pyrrolidine)-tetra-malonate Hexa-Adducts of C_{60} : The Unexpected Regio- and Stereocontrol Mediated by Malonate–Pyrrolidine Interaction Edison Castro,^[a] Khalid Azmani,^[b] Andrea Hernandez Garcia,^[a] Amineh Aghabali,^[c] Shuming Liu,^[a] Alejandro J. Metta-Magana,^[a] Marilyn M. Olmstead,^{*,[d]} Antonio Rodríguez-Fortea,^[b] Josep M. Poblet,^{*,[b]} and Luis Echegoyen^{*,[a]}

Abstract: A totally unanticipated regio- and stereoisomerically pure C_{2h} -symmetric *trans*-1-(bis-pyrrolidine)-tetra-malonate hexa-adduct of C_{60} was obtained via a topologically controlled method, followed by a 1,3-dipolar cycloaddition reaction. The structures of the products were elucidated by

^1H and ^{13}C NMR and by X-ray crystallography. The unexpected regio- and stereoselectivity observed, supported by theoretical calculations, was found to be a consequence of malonate–pyrrolidine interactions.

Introduction

The chemical and physical properties of fullerenes and their derivatives are mainly the result of their unique electron accepting abilities and high charge transport capabilities in three dimensions.^[1] The presence of thirty equivalent [6,6] double bonds on the C_{60} carbon cage, all of which exhibit identical reactivity, results in low regioselectivity of multiple addition products. After monoadduct formation, subsequent additions of one, two, or three symmetrical addends can yield 8, 46, and 262 possible regioisomers, respectively.^[2,3] 1,3-dipolar cycloaddition reactions of azomethine ylides to C_{60} have been extensively studied and it is one of the most powerful and versatile methods for derivatizing fullerenes.^[4] Prato and co-workers found that all eight possible bis-adduct regioisomers were obtained upon 1,3-dipolar cycloaddition to C_{60} when the azomethine ylide is symmetric,^[5] showing that this reaction is less

chemoselective than cyclopropanations of C_{60} .^[6] The purification of regioisomers by column chromatography is challenging because the bis-adducts exhibit similar polarities.^[7]

There are two well-known methods to reduce the number of regio-isomers of C_{60} and C_{70} derivatives, the tether-directed remote multifunctionalization introduced by Diederich et al.,^[8] and the topologically controlled method introduced by Kräutler et al.^[9] Both methods have been widely used to synthesize bis-, tris-, tetra-, penta- and hexa-derivatives of C_{60} .^[10–12]

Martin and co-workers reported a straightforward procedure catalyzed by silver or copper acetate to efficiently obtain pyrrolidino[60]fullerenes with stereochemical control by enantioselective cycloaddition of N-metalated azomethine ylides to C_{60} .^[13,14] This methodology was later extended to higher fullerenes and endohedral fullerenes.^[15] Ovchinnikova and co-workers reported an efficient metal-assisted azomethine ylide cycloaddition method for the diastereoselective synthesis of 5-substituted 3,4-fulleroproline esters based on the lithium salt-assisted cycloaddition of azomethine ylides.^[16] In contrast to the thermal reactions that often result in the formation of diastereomeric mixtures of products, metal-mediated azomethine ylide cycloaddition at low temperature leads to higher yields and diastereoselectivity. However, this kind of reaction has been scarcely studied.


Here, we report a regio- and stereoselective synthesis of hybrid fullerene C_{60} hexa-adducts using a combination of a Diels–Alder reaction, followed by an addition–elimination of bromoethylmalonate, then a retro-Diels–Alder and finally by a 1,3-dipolar cycloaddition reaction of azomethine ylides. Surprisingly, only one regio- and stereoselective product corresponding to the isomer *cis-anti-cis* hexa-adduct (see Figure 3 for structural nomenclature) was observed. The final products were fully characterized by matrix assisted laser desorption/ionization time-of-flight mass spectroscopy (MALDI-TOF-MS),

[a] E. Castro, A. H. Garcia, Dr. S. Liu, Dr. A. J. Metta-Magana, Prof. Dr. L. Echegoyen
Department of Chemistry, University of Texas at El Paso
500W University Avenue, El Paso, Texas, 79902 (USA)
E-mail: echegoyen@utep.edu

[b] K. Azmani, Dr. A. Rodríguez-Fortea, Prof. Dr. J. M. Poblet
Departament de Química Física i Inorgànica
Universitat Rovira i Virgili, C/Marcel·lí Domingo 1, 43007 Tarragona (Spain)
E-mail: josepmaria.poblet@urv.cat

[c] Dr. A. Aghabali
Department of Chemistry and Biochemistry
California Polytechnic State University, San Luis Obispo, California (USA)

[d] Prof. Dr. M. M. Olmstead
Department of Chemistry, University of California at Davis
One Shields Ave, Davis, California, 95616 (USA)
E-mail: mmolmstead@ucdavis.edu

 Supporting information and the ORCID identification numbers for the authors of this article can be found under <https://doi.org/10.1002/chem.201702866>.

^1H and ^{13}C NMR spectroscopy and X-ray crystallography. The overall regio- and stereoselectivity observed was explained by theoretical calculations.

Results and Discussion

Synthesis and NMR studies of 2, 3, 6 and 7

The C_{60} -(*e,e,e,e*)-tetra-malonate (C_{60} -TM) (Figure 1 a) was synthesized following a procedure previously reported.^[17] Penta-adduct **2** and hexa-adduct **3** were synthesized by reacting C_{60} -

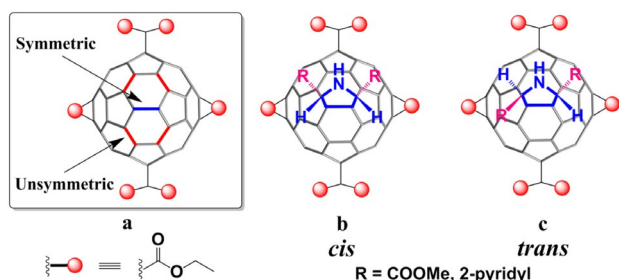
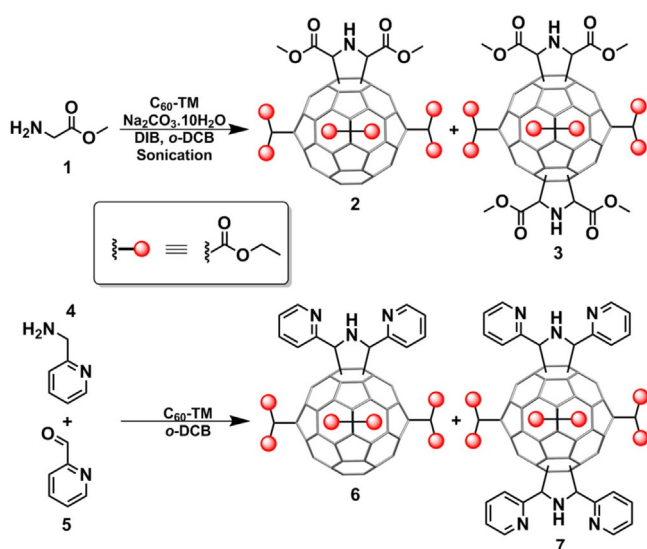


Figure 1. a) symmetric and unsymmetric double bonds, b) symmetric *cis* addition, c) symmetric *trans* addition.

TM with methyl glycine ester in the presence of diacetoxyiodobenzene (DIB) and sodium carbonate decahydrate in *ortho*-dichlorobenzene (*o*-DCB) under sonication at room temperature (Scheme 1). After 30 minutes the solution turned orange and compound **2** was the major product, however after 3 h the solution turned yellow and compound **3** was the main product as monitored by TLC using a dichloromethane/ethyl acetate (DCM/EtOAc) 30:1 mixture as the eluent. After column chromatographic purification compounds **2** and **3** were characterized by MALDI-TOF-MS and NMR spectroscopy.

The molecular-ion peaks for the penta- and hexa-adduct compounds at m/z 1511.282 and 1670.341, were observed by



Scheme 1. Synthesis of penta-adducts **2** and **6** and hexa-adducts **3** and **7**.

MALDI-TOF-MS, respectively (Figure S1). Because the azomethine ylide can add to the symmetric or unsymmetric bonds (Figure 1 a), two regioisomers are possible for the penta-adduct. Surprisingly, only one isomer was observed, and by ^1H and ^{13}C NMR and X-ray crystal structure a C_s symmetry was assigned to compound **2**.

The ^1H NMR spectrum of **2** (Figure 2 a) exhibits only one set of signals for the pyrrolidine addend ($\delta=4.69$, 3.89, and 3.76 ppm), clearly establishing the presence of a plane of symmetry, indicating that the addition must have occurred on the symmetric bond (Figures 1 b and 1 c). The C_s symmetry of compound **2** was also confirmed by the ^{13}C NMR spectrum (Figure 2 b). Five resonances for carbonyl groups at $\delta=169.0$ (ester groups of the pyrrolidine addend), 163.8 ($\times 2$), 163.7 and 163.4 ppm (four malonates), five resonances for the methyl groups at $\delta=52.9.0$ (methyl groups of the pyrrolidine addend), 14.2 ($\times 2$) and 14.1 ($\times 2$) ppm (four malonates) indicate that the four malonate groups are in different chemical environments.

Twenty four ^{13}C resonances between $\delta=138.0$ and 152.2 ppm were observed for the sp^2 carbons of the fullerene cage, two resonances at $\delta=76.0$ and 72.1 ppm from the pyrrolidine ring, and four resonances at $\delta=63.1 \times 2$, 63.0 and 62.7 ppm assigned to the methylene groups, in agreement with the four resonances expected for the methylene groups.

Finally, the stereospecific *cis*-addition (Figure 1 b) was unambiguously established by the six sp^3 signals observed for the fullerene carbon atoms at $\delta=69.9$, 69.8, 69.5, 69.3, 45.5, and 45.1 ppm and the three sp^3 signals for the carbons of the four cyclopropane rings at $\delta=67.8$, 67.5, and 44.8 ppm (Figure 2 b). If the *trans*-addition had occurred (Figure 1 c) only four sp^3 signals for the fullerene carbon atoms and two sp^3 signals for the cyclopropane rings would have been observed.

Compound **3** was identified as the hexa-adduct with the pyrrolidines in a *trans*-1 relative position, as shown in Figure 3. The ^1H NMR of compound **3** (Figure 4 a) exhibits only one set of signals for the two pyrrolidines ($\delta=4.90$, 3.82, and 3.69 ppm), showing the presence of a plane of symmetry, which is only possible if the second addition has occurred on the *trans*-1 position. Figures 3 a–e show front and side views for the five possible *trans*-1 isomers, where the first and third descriptors refer to the pyrrolidine stereochemistry and the middle one refers to their relative orientation. For example, *cis-anti-cis* refers to the two substituents on the pyrrolidine being in a *cis* position but with an *anti* orientation with respect to the other pyrrolidine substituents (Figures 3 a, front and side view).

The ^{13}C NMR spectrum of compound **3** (Figure 4 b) showed twelve resonances for the sp^2 carbons of the fullerene cage between $\delta=152.3$ –139.1 ppm, two resonances for the pyrrolidines at $\delta=74.0$ and 72.9 ppm, one resonance for the methoxy groups at $\delta=52.8$ ppm, two resonances at $\delta=66.4$ and 44.4 ppm for the cyclopropane carbon-bridged atoms, two resonances for the methylene groups and two for the methyl groups of the malonates at $\delta=63.0$, 62.5 and $\delta=14.1 \times 2$, respectively.

Surprisingly, only three carbonyl group resonances were observed, one at $\delta=169.4$ ppm, assigned to the carbonyl groups

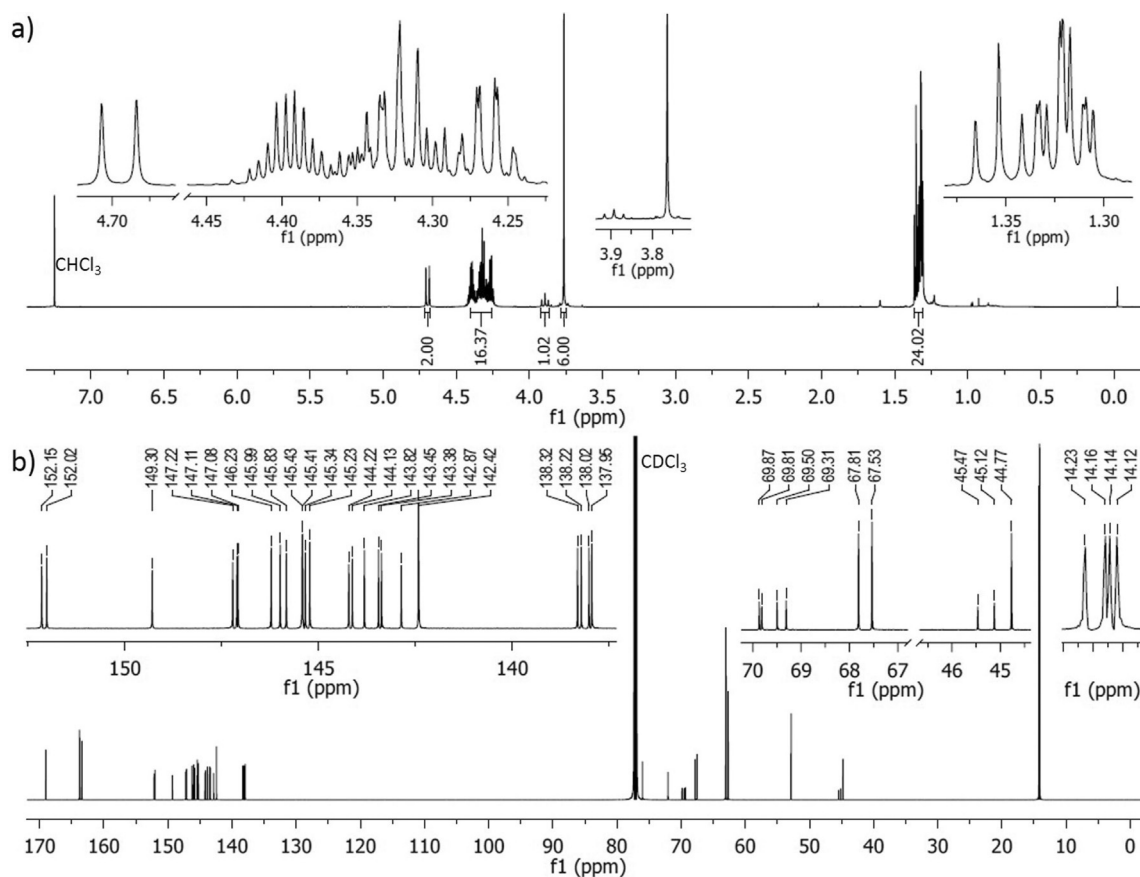


Figure 2. ^1H and ^{13}C NMR of compound 2, (CDCl_3).

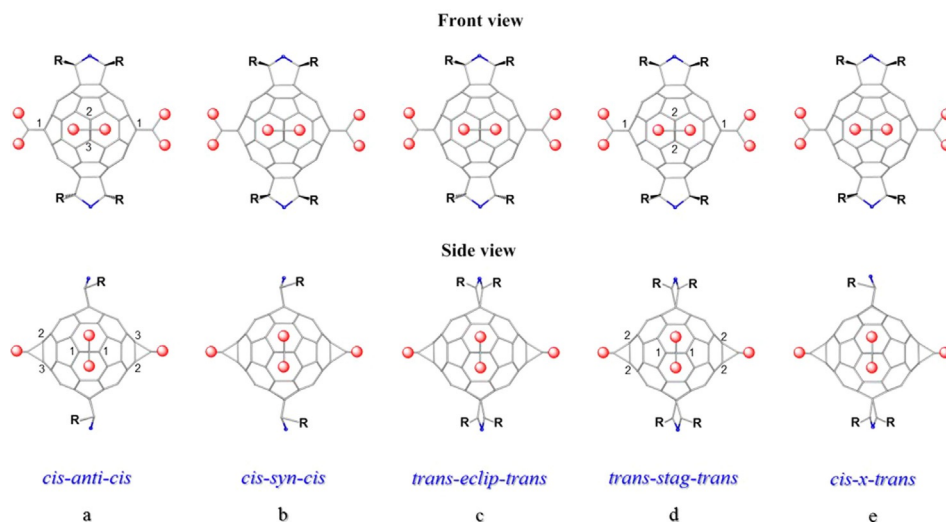


Figure 3. Front and side view of the possible hexa-adduct stereoisomers of C_{60} (compounds 3 and 7) taking into account only *trans*-1 additions of the azomethine ylides to C_{60} -TM. The red balls represent ethoxycarbonyl groups.

of the pyrrolidine addends and two at $\delta = 163.5$ and 163.4 ppm, assigned to the carbonyl groups of the four malonates.

These observations are consistent with one of two possible structures, one where the pyrrolidines are both *cis* but *anti* relative to each other (Figure 3a), or one where the groups in the

pyrrolidine are *trans* but the two pyrrolidines are staggered (Figure 3d). For structures 3b, 3c and 3e four resonances for the carbonyl groups are expected (one for the carbonyl groups of the pyrrolidines and three for the carbonyls of the malonates). The sp^3 resonances from the cyclopropane carbon atoms were crucial to unambiguously identify the structure of

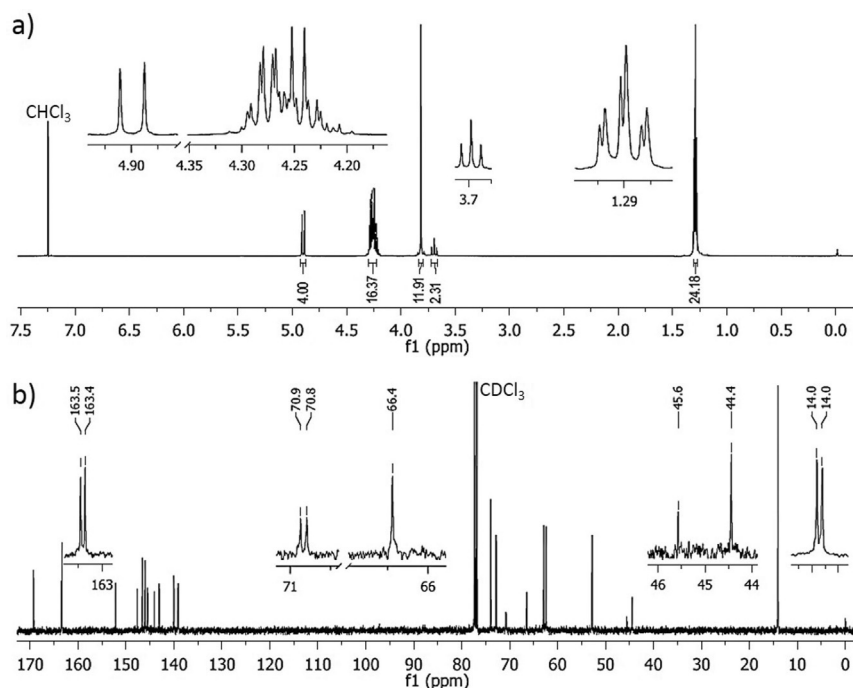


Figure 4. ^1H and ^{13}C NMR of compound **3**, (CDCl_3).

compound **3**. Three resonances at $\delta = 70.9$, 70.8 and 45.6 ppm clearly prove that the *cis-anti-cis* isomer (Figure 3 a) was the product obtained, since only two resonances would be observed for the *trans-stag-trans* isomer, as shown in Figure 3 d.

In view of the surprising and unprecedented regio- and stereoselectivity observed for compound **3**, we decided to study this reaction using a different substituent (2-pyridyl) on the pyrrolidine addends (compound **7**) (Scheme 1).

Hexa-adduct **7** was synthesized by reacting C_{60} -TM with 2-picolylamine (**4**) and 2-pyridinecarbaldehyde (**5**) in *o*-DCB, under reflux for 30 min.

After 30 min the solution turned yellow, and the main product, compound **7**, was purified by silica gel column chromatography using a chloroform/methanol ($\text{CHCl}_3/\text{MeOH}$) 15:1 mixture. The reaction was monitored by TLC using the same mixture of solvents. The isolated product **7** was characterized by MALDI-TOF-MS and by NMR spectroscopy.

The MALDI-TOF-MS confirmed the presence of the molecular-ion peak for the hexa-adduct derivative at m/z 1746.425 (Figure S4). NMR analyses similar to those conducted with compound **3** confirmed the regio- and stereoselectivity of the C_{2h} -symmetric *trans-1* addition of compound **7**, as for compound **3**.

The ^1H NMR spectrum of compound **7** (Figure S5a) shows a doublet at $\delta = 5.52$ ppm, which corresponds to the four identical pyrrolidine protons. Four signals in the aromatic region were assigned to the 2-pyridyl groups and a triplet at $\delta = 5.06$ ppm was assigned to the NH of the pyrrolidine addends. One ABX_3 and one AMX_3 system were observed for the methylene groups of the four malonates at $\delta = 4.25$ and 4.12 ppm, respectively (Figure S5a). Two triplets at $\delta = 1.28$ and 1.22 ppm

reflect the different chemical environments of the methyl groups of the four malonates.

The ^{13}C NMR spectrum (Figure S5b) of compound **7** showed similar resonances to those of compound **3**. Two resonances for the carbonyl groups at $\delta = 163.8$ and 163.4 ppm, seventeen resonances between 156.1 and 122.6 ppm (twelve resonances for the sp^2 fullerene carbon atoms and five for the 2-pyridyl groups), two resonances for the pyrrolidine addends at $\delta = 70.6$ and 76.5 ppm, two resonances for the methylene groups at $\delta = 62.7$ and 62.1 ppm, and two resonances for the methyl groups at $\delta = 14.1$ ppm. Finally, five resonances at $\delta = 72.7$, 70.9 , 66.2 , 45.4 , and 44.1 ppm prove the presence of the *cis-anti-cis* isomer.

Crystallography studies

To further support the assigned regio- and stereochemistry of compound **2**, crystals were grown by slow evaporation in toluene. The crystal structure of compound **2**, (Figure 5 a) clearly shows a plane of symmetry and confirms the *cis* orientation of the two substituents (ester groups at C61 and C64) in the pyrrolidine. The C1–C2 (Figure 5 a) distance is $1.590(3)$ Å, longer than the typical 6:6 distance of 1.38 Å in pristine C_{60} .

Crystal data for **2**: $a = 12.9239(7)$, $b = 13.9988(7)$, $c = 20.5853(11)$ Å, $\alpha = 88.077(2)$, $\beta = 74.686(2)$, $\gamma = 65.018(2)^\circ$, $U = 3243.0(3)$ Å³, $T = 100$ K, red blocks, space group $P\bar{1}$ (no. 2), $Z = 2$, 35340 reflections measured, 14518 unique ($R_{\text{int}} = 0.031$), $R_1(I > 2\sigma(I)) = 0.0494$, $wR_2(\text{all data}) = 0.1309$.

We failed in our attempts to grow single crystals of compound **7** using different solvents such as toluene, chloroform and dichloromethane. A variety of functionalized terpyridines have been complexed using different metals including Zn,^[18,19]

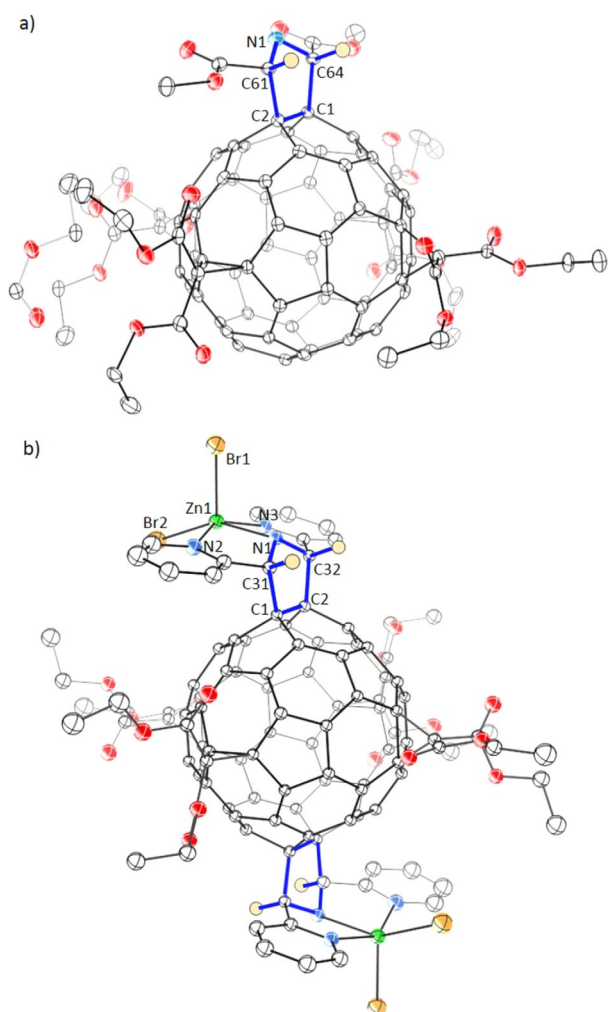


Figure 5. Crystal structure of a) compound **2** and b) compound **7** complexed with ZnBr_2 . Atoms labelled C1 and C2 are part of the C_{60} and are symmetrically placed at a 6:6 junction. Atoms are drawn with thermal ellipsoids at the 50% probability level. For clarity, the pyrrolidine bonds are shown in blue, the hydrogens in the *cis* position are yellow, the bromines are gold and the zincs are green.

therefore, crystals of compound **7** were grown by complexation with ZnBr_2 by slow evaporation in a benzene/chloroform/ethanol (9:9:1) mixture (Figure 5 b).

The X-ray crystallography data shows a discrete molecule where compound **7** was complexed with two molecules of ZnBr_2 . These results confirm the exclusive observation of the *cis-anti-cis* structure. The crystallographic inversion center found in the structure of **7** confirms that two pyrrolidines are in a relative *trans-1* orientation. The pyridyl substituents at C31 and C32 are in a *cis* orientation, yet they are *anti* with respect to the other pyrrolidine substituents (Figure 5 b).

The coordination geometry at Zn1 is intermediate between trigonal bipyramidal and square pyramidal. The C1–C2 (Figure 5 b) 6:6 bond distance is 1.587(5) Å. Crystal data for **7**: $a = 14.8721(7)$, $b = 13.3913(7)$, $c = 27.1851(12)$ Å, $\beta = 104.206(3)^\circ$, $U = 5248.5(4)$ Å³, $T = 100$ K, yellow needles, space group $P2_1/n$ (no. 14), $Z = 2$, 72431 reflections measured, 12022 unique ($R_{\text{int}} = 0.083$), $R_1(I > 2\sigma(I)) = 0.0604$, wR_2 (all data) = 0.1597.

Details of the solution and refinement of the structures are available in the crystallographic information files (CIF).

Computational analysis

DFT calculations were performed to try to understand the reasons for the selective formation of the *cis-anti-cis* isomers (Scheme 1). To understand the different factors that govern the stereoselectivity for this kind of reactions, the addition of one azomethine ylide to form the mono-pyrrolidine penta-adduct was initially studied. Afterwards, the possible isomers of the bis-pyrrolidine hexa-adducts were analyzed.

The mono-pyrrolidine penta-adduct. *Cis* (**1b**) and *trans* (**1c**) pyrrolidine groups can result from the conformation of the azomethine ylide, which can exist in a *W*- or *S*-shape.^[20] Cycloadditions of azomethine ylides to C_{60} show differences around 1–2 kcal mol⁻¹ in favor of the *cis* conformation.^[20]

The slightly higher stability of the *cis* versus the *trans* isomer is mainly due to the deformation degree of the pyrrolidine addend. DFT calculations were carried out to find the reaction energies of the 1,3-dipolar cycloaddition of azomethine ylide to C_{60} , *e,e,e,e*-(tetramethylene)- C_{60} ((CH_2)_{4 C_{60}) and C_{60} -TM models. Values in Table 1 show higher reaction energies for C_{60} -TM than that of C_{60} and (CH_2)₄ C_{60} models. Furthermore, stabilization of the *cis* versus the *trans* conformation is enhanced from energy differences of 1–2 kcal mol⁻¹ to 2–4 kcal mol⁻¹.}

Table 1. Bonding energies (BE, in the gas phase) and MAI values of the mono-pyrrolidine adducts (ester and pyridyl-substituted) with C_{60} , (CH_2)₄ C_{60} model and C_{60} -TM.^[a]

BE	Ester		Pyridyl	
	<i>cis</i> (1b)	<i>trans</i> (1c)	<i>cis</i> (1b)	<i>trans</i> (1c)
C_{60}	–28.8	–27.9	–30.8	–28.8
(CH_2) ₄ C_{60}	–27.2	–26.3	–28.5	–26.4
C_{60} -TM	–31.8	–30.1	–34.2	–30.4
MAI ^[b]	–4.6	–3.8	–5.7	–4.0

[a] All energy values are expressed in kcal mol⁻¹. [b] Malonate–pyrrolidine adduct interactions are calculated as $\text{MAI} = \text{BE}[\text{pa-C}_{60}\text{-TM}] - \text{BE}[\text{pa-(CH}_2)_4\text{C}_{60}]$.

These results can be explained by the different interactions between the malonate groups and the pyrrolidine adduct in each of the two isomers (vide infra).

The malonate–pyrrolidine adduct interaction (MAI) was quantified as the difference between the bonding energy (BE) of the pyrrolidine adduct (pa) in C_{60} -TM and that in the (CH_2)₄ C_{60} model, where the four malonates are replaced by four methylene groups, $\text{MAI} = \text{BE}[\text{pa-C}_{60}\text{-TM}] - \text{BE}[\text{pa-(CH}_2)_4\text{C}_{60}]$. This definition assumes that there are no interaction between the pyrrolidine adduct and the methylenes in the reference (CH_2)₄ C_{60} compound.

The MAI values range between –4 and –6 kcal mol⁻¹ (see values in Table 1) for the *trans* and *cis* isomers of the ester- and pyridyl-substituted pyrrolidine adducts, meaning that there is a non-negligible attractive interaction between the

equatorial malonates and the substituents of the pyrrolidine addend. To verify this result, we also considered a simplified model system composed only of the pyrrolidine and the malonates (no carbon cage, see Figure S7), to calculate the interaction energies between these groups (pyrrolidine–malonates) for the *cis* isomers of the ester- and pyridyl–pyrrolidine adducts. The calculated interaction energies are very similar to the MAI values, confirming the validity of the latter as a measure of this interaction (see values in Table S2).

To gain additional insight into the nature of the interaction between the pyrrolidine ends and the malonates, we performed calculations for some of the fragment models without taking into account the dispersion corrections (see Table S2 and Figure S7). The results, which show positive, that is, repulsive, interaction energies confirm that the attractive interactions results from dispersion forces between the pendant groups in the malonates and the pyrrolidine.

We also found that the pyrrolidine–malonate interactions critically depend on the addition position of the malonate chains. There are two types of malonate addends as a result of *e*-face and *e*-edge additions (Figure 6). The *e*-edge malonates,

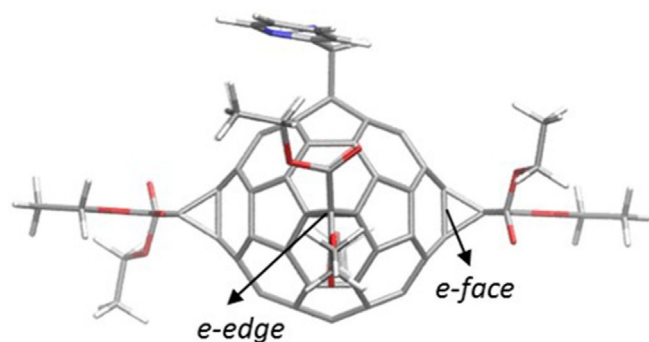


Figure 6. Optimized structure of mono-(pyridyl-pyrrolidine) penta-adduct of C_{60} .

are closer to the pyrrolidine group than the *e*-face ones, thus resulting in a significantly larger interaction. Indeed, calculations using a series of pyrrolidino C_{60} -dimalonate models confirm that the *e*-edge addends are mainly responsible for the total pyrrolidine–malonates interaction (Tables S2 and S3).

Calculations were also carried out in *o*-DCB, which was the solvent used in the experiments. Both the position and the geometry of the malonate chains were slightly affected by the solvent, therefore the interaction between the malonates and the pyrrolidine groups was also affected. The results still show the stabilization due to the interaction between the pyrrolidine groups and the malonates already found in the gas phase calculations. Interestingly, a different trend was observed depending on the pyrrolidine group substituents. For the ester group, the value of the MAI, $-2.1 \text{ kcal mol}^{-1}$, is affected drastically, decreasing by half in comparison with the gas phase value, while for the pyridyl compound the MAI, $-5.3 \text{ kcal mol}^{-1}$, does not change appreciably. These results reflect to the free space available between the pyrrolidine group and the malonate

chains that is accessible to solvent molecules. The bulkier and less flexible the pyrrolidine group, the smaller the space for the solvent to access the region between the malonate and the pyrrolidine, therefore the smaller the change of the MAI in the gas phase. If the regions of the malonate and the pyrrolidine that interact through dispersion forces are more effectively solvated, their attractive interactions are decreased and the MAI is reduced.

The bis-pyrrolidine hexa-adduct. The different stereoisomers resulting from the second 1,3-dipolar cycloaddition on the symmetric bond (Figure 3) can be classified into two sets. On one hand, there are those isomers with two *cis*-pyrrolidine groups (Figure 3 a and b), and on the other, those isomers with at least one *trans* group (Figure 3 c, d and f). The *trans* conformation of the pyrrolidine group results in a destabilization relative to the *cis* conformation. The second set of isomers, which contains at least one *trans*-pyrrolidine group, is around 3–7 kcal mol^{-1} higher in energy than the first set (see values in Table 2). In general, the higher the number of *trans* groups, the larger the destabilization. However, the results do not show a strictly additive effect.

Table 2. Binding energies (BE), relative energies (ΔE , gas phase and solvent) with MAI values (in parenthesis), free energies and percentage for different C_{60} hexa-adducts.^[a]

Group	Iso	<i>cis/trans</i>	BE gas	ΔE gas	ΔE solv ^[b]	ΔG ^[c]	Iso % ^[c]
Ester	3a	2/0	-61.4	0.0 (-8.9)	0.0 (-3.4)	0.0	75.8
	3b	2/0	-61.2	0.2 (-8.8)	0.5 (-3.0)	0.9	16.8
	3c	0/2	-59.9	4.5 (-6.3)	3.2 (-2.3)	2.1	2.4
	3d	0/2	-59.0	2.4 (-8.2)	1.1 (-4.2)	2.1	2.3
	3e	1/1	-58.4	3.0 (-6.6)	2.6 (-1.4)	2.0	2.7
Pyridyl	3a	2/0	-63.5	1.1 (-8.9)	0.0 (-7.5)	0.0	98.3
	3b	2/0	-64.6	0.0 (-10.0)	0.7 (-6.8)	2.4	1.7
	3c	0/2	-58.4	6.2 (-8.0)	7.3 (-4.7)	8.2	0.0
	3d	0/2	-57.9	6.8 (-7.5)	6.5 (-5.4)	5.0	0.0
	3e	1/1	-61.0	3.7 (-8.4)	3.2 (-6.6)	4.9	0.0

[a] Energies in kcal mol^{-1} . [b] *o*-DCB. [c] At 300 K.

Looking at the first set of isomers, the energy differences between isomers **3a** and **3b** are rather small. The only difference between these two isomers is the relative position of the two *cis*-pyrrolidine groups, which can be either in a *syn* or in a *anti* position relative to each other (Figure 3). In the case of the pyridyl–pyrrolidine group, **3b** (*syn*) is slightly lower in energy than **3a** (*anti*). For the ester–pyrrolidine group, the two isomers are almost degenerate, with **3a** (*anti*) being only $0.2 \text{ kcal mol}^{-1}$ lower in energy than **3b** (*syn*). These small differences are exclusively a consequence of the presence of the malonate chains as the same systems without malonates are degenerate (see Table S4). These energy differences are essentially kept when using hybrid methods (see Table S5).

As for the mono-pyrrolidine penta-adduct, we calculated the MAI for **3a–e** (see Table 2). The results are around two times those of the penta-adduct. For the ester-pyrrolidine penta-adduct **1b** the MAI is $-4.6 \text{ kcal mol}^{-1}$ and for the hexa-adduct **3a** it is $-8.9 \text{ kcal mol}^{-1}$ (Table 2). Therefore, the MAI value is

the result of additive independent interactions for each of the two pyrrolidine adducts with the malonate chains.

As found for the penta-adduct, solvent is a crucial factor to compute the malonate–pyrrolidine interaction, which can be seen as the driving force for the formation of these compounds. The solvent affects the malonate chains, and solvates the adducts, reducing the strength of this interaction. Stabilization of the **3a** (*anti*) isomer, which is the one obtained experimentally, with respect to **3b** (*syn*) is enhanced when *o*-DCB is present. For the ester–pyrrolidine group, an increase of the energy difference between the two isomers is found (from 0.2 to 0.5 kcal mol⁻¹). For the pyridyl–pyrrolidine isomers, an inversion of relative stability is observed (see Table 2). Furthermore, the MAI values are affected by the solvent in the same way as for the penta-adduct.

The different interactions with the solvent helps to explain the stabilization of **3a** with respect to **3b**. The optimized structures show that the malonate chains in **3a** are compact and close to the pyrrolidine groups. However, in **3b** they tend to be farther from the pyrrolidine groups and thus easier to be solvated, consequently reducing the interaction strength with the pyrrolidine groups (Figure 7). This effect is quite critical for the pyridyl–pyrrolidine derivative where the MAI value for **3a** (−6.8 kcal mol⁻¹) is rather similar to that of the mono-pyrrolidine penta-adduct (−5.3 kcal mol⁻¹).

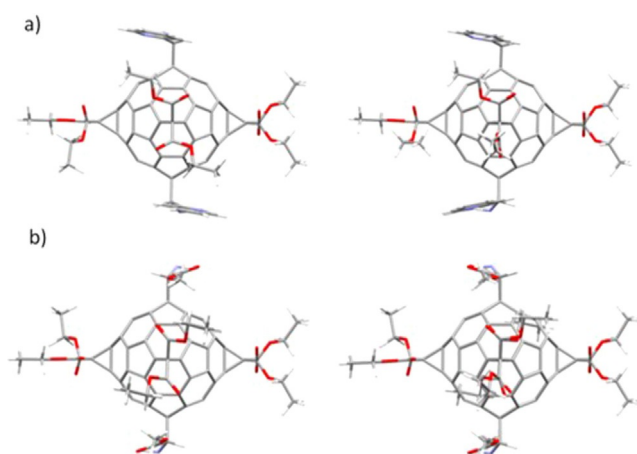


Figure 7. Optimized structure in *o*-DCB of *anti* and *syn* isomers of a) pyridyl-substituted and b) ester-substituted bis-pyrrolidine hexa-adducts of C₆₀.

Finally, we have computed the free energies, within the rigid rotor and harmonic oscillator (RRHO) approximation, at the temperature and pressure conditions of the experiment. The results show that isomer **3a** is favored with respect to **3b**, by up to almost 1 kcal mol⁻¹ for the ester- and 2.4 kcal mol⁻¹ for the pyridyl–pyrrolidine. This relative stabilization is governed mainly by the entropic contribution. We also computed the free energy for the other three isomers **3c**, **3d** and **3e**. For the pyridyl-substituted hexa-adduct, the relative free energies for **3c–e** are rather high compared to that for **3a** (more than 5 kcal mol⁻¹, see Table 2). For the ester-substituted hexa-adduct,

however, the free energy differences are not so large, in line with their energy differences (see Table 2).

Such differences in the free energies lead to relative abundances for the *cis-anti-cis* (**3a**) versus *cis-syn-cis* (**3b**) stereoisomers at experimental conditions of 76 versus 17% for the ester group and 98 versus 2% for the pyridyl group, in good agreement with experiments. The percentages for the rest of isomers **3c–e** are small for the ester group (around 2%) and negligible for the pyridyl group (0%).

Conclusions

We have synthesized a new hexa-adduct derivative of C₆₀ by a 1,3-dipolar cycloaddition reactions via two different conditions and using C₆₀-TM as the starting material. These reactions are highly regio- and stereoselective, surprisingly leading to the exclusive formation of the *cis-anti-cis* isomer. The formation of the *cis-anti-cis* hexa-adduct isomers as the only observed products was mainly attributed to the interaction between the pendant groups in the malonate and the pyrrolidine groups. This interaction, which is very important in the gas phase (van der Waals type), is attenuated in the presence of the solvent (*o*-DCB). Determination of the free energies allowed the estimation of the relative abundances of the *cis-anti-cis* and *cis-syn-cis* hexa-adducts, confirming that the former predominates under the experimental conditions.

Experimental Section

Synthesis of C₆₀-TM

C₆₀-TM was synthesized following a procedure previously reported.^[17]

Synthesis of compounds 2 and 3

Penta-adduct **2** and hexa-adduct **3** were synthesized by reacting C₆₀-TM (50 mg, 0.04 mmol) with methyl glycine ester hydrochloride (20 mg, 0.16 mmol) in the presence of diacetoxyiodobenzene (39 mg, 0.12 mmol) and sodium carbonate decahydrated (37 mg, 0.13 mmol) in *o*-DCB (10 mL), under sonication at room temperature and covered from light. After 30 min the solution turned orange and compound **2** was the major product, however after 3 h the solution turned yellow and compound **3** was the main product as monitored by TLC using DCM/EA 30:1 mixture, as the eluent. After column chromatography purification compounds **2** and **3** were characterized by MALDI-TOF-MS and NMR spectroscopy.

Synthesis of compound 7

Hexa-adduct **7** was synthesized by reacting C₆₀-TM (50 mg, 0.04 mmol) with 2-picolylamine (17 mg, 0.16 mmol) and 2-pyridinecarbaldehyde (17 mg, 0.16 mmol) in *o*-DCB (10 mL), under reflux. After 30 min the solution turned yellow and compound **7** was the only product as monitored by TLC using CHCl₃/MeOH 15:1 mixture, as the eluent. After column chromatography purification compound **7** was characterized by MALDI-TOF-MS and NMR spectroscopy.

Computational details

The theoretical study of the 1,3-dipolar cycloaddition reactions of azomethine ylides has been performed by DFT methodology using ADF2016 code.^[21,22] An exhaustive exploration of the potential products was performed including the relative arrangements of malonates with respect to pyrrolidine groups (See Figure 1 and Table S1). The exchange-correlation GGA density functional of Becke and Perdew (BP86) were employed to calculate all the minima.^[23,24] Relativistic corrections were included by means of the ZORA (the Zeroth Order Regular Approximation) formalism.^[25–27] Dispersion corrections were also incorporated (D3 method by Grimme)^[28] Solvent effects were included via the conductor-like screening model (COSMO) using Solvent Excluded Surface (SES).^[29,30] Slater Basis sets of TZP quality were used to describe the valence electrons of H, C, N and O. Frozen cores of C, N and O were described by means of single Slater functions.

Acknowledgements

L.E. thanks the US National Science Foundation (NSF) for generous support of this work under the NSF-PREM program (DMR 1205302) and the CHE-1408865. The Robert A. Welch Foundation is also gratefully acknowledged for an endowed chair to L.E. (Grant AH-0033). This work was also supported by the Spanish Ministerio de Ciencia e Innovación (Project No. CTQ2014-52774-P) and the Generalitat de Catalunya (2014SGR-199 and XRQTC). J.M.P. thanks the ICREA foundation for an ICREA ACADEMIA award. M.M.O. and A.A. thank Beamline 11.3.1 at the Advanced Light Source synchrotron facility. The Advanced Light Source is supported by the Director, Office of Science, Office of Basic Energy Sciences, of the US Department of Energy under Contract No. DE-AC02-05CH11231.

Conflict of interest

The authors declare no conflict of interest.

Keywords: fullerenes · hexa-adducts · malonates · regiochemistry · stereochemistry

- [1] A. Hirsch, in *Fullerenes and Related Structures*, Vol. 199, Springer, Heidelberg, 1999, pp. 1.
 [2] L. Pasimeni, A. Hirsch, I. Lamparth, A. Herzog, M. Maggini, M. Prato, C. Corvaja, G. Scorrano, *J. Am. Chem. Soc.* **1997**, *119*, 12896.

- [3] P. W. Fowler, *J. Chem. Soc. Faraday Trans.* **1995**, *91*, 2241.
 [4] U. Ortiz-Méndez, in *Handbook of Less-Common Nanostructures*, CRC, **2012**, p.623.
 [5] K. Kordatos, S. Bosi, T. Da Ros, A. Zambon, V. Lucchini, M. Prato, *J. Org. Chem.* **2001**, *66*, 2802.
 [6] S. Bosi, T. Da Ros, G. Spalluto, J. Balzarini, M. Prato, *Bioorg. Med. Chem. Lett.* **2003**, *13*, 4437.
 [7] Q. Lu, D. I. Schuster, S. R. Wilson, *J. Org. Chem.* **1996**, *61*, 4764.
 [8] L. Isaacs, R. F. Haldimann, F. Diederich, *Angew. Chem. Int. Ed. Engl.* **1994**, *33*, 2339; *Angew. Chem.* **1994**, *106*, 2434.
 [9] B. Kräutler, T. Müller, J. Maynollo, K. Gruber, C. Kratky, P. Ochsenbein, D. Schwarzenbach, H.-B. Bürgi, *Angew. Chem. Int. Ed. Engl.* **1996**, *35*, 1204; *Angew. Chem.* **1996**, *108*, 1294.
 [10] M. R. Cerón, M. Izquierdo, Y. Pi, S. L. Atehortúa, L. Echegoyen, *Chem. Eur. J.* **2015**, *21*, 7881.
 [11] M. J. van Eis, R. J. Alvarado, L. Echegoyen, P. Seiler, F. Diederich, *Chem. Commun.* **2000**, 1859.
 [12] S. Zhang, O. Lukyanova, L. Echegoyen, *Chem. Eur. J.* **2006**, *12*, 2846.
 [13] E. E. Maroto, A. de Cózar, S. Filippone, Á. Martín-Domenech, M. Suarez, F. P. Cossío, N. Martín, *Angew. Chem. Int. Ed.* **2011**, *50*, 6060; *Angew. Chem.* **2011**, *123*, 6184.
 [14] E. E. Maroto, S. Filippone, A. Martín-Domenech, M. Suarez, N. Martín, *J. Am. Chem. Soc.* **2012**, *134*, 12936.
 [15] E. E. Maroto, M. Izquierdo, S. Reboredo, J. Marco-Martínez, S. Filippone, N. Martín, *Acc. Chem. Res.* **2014**, *47*, 2660.
 [16] V. A. Ioutsí, A. A. Zadorin, P. A. Khavrel, N. M. Belov, N. S. Ovchinnikova, A. A. Goryunkov, O. N. Kharybin, E. N. Nikolaev, M. A. Yurovskaya, L. N. Sidorov, *Tetrahedron* **2010**, *66*, 3037.
 [17] R. Schwenninger, T. Müller, B. Kräutler, *J. Am. Chem. Soc.* **1997**, *119*, 9317.
 [18] H. Hofmeier, U. S. Schubert, *Chem. Soc. Rev.* **2004**, *33*, 373.
 [19] A. D'Aléo, E. Cecchetto, L. De Cola, R. Williams, *Sensors* **2009**, *9*, 3604.
 [20] G. Pandey, P. Banerjee, S. R. Gadre, *Chem. Rev.* **2006**, *106*, 4484.
 [21] C. Fonseca Guerra, J. G. Snijders, G. te Velde, E. J. Baerends, *Theor. Chem. Acc.* **1998**, *99*, 391.
 [22] G. te Velde, F. M. Bickelhaupt, E. J. Baerends, C. Fonseca Guerra, S. J. A. van Gisbergen, J. G. Snijders, T. Ziegler, *J. Comput. Chem.* **2001**, *22*, 931.
 [23] A. D. Becke, *Phys. Rev. A* **1988**, *38*, 3098.
 [24] A. D. Becke, *J. Chem. Phys.* **1993**, *98*, 5648.
 [25] E. v. Lenthe, E. J. Baerends, J. G. Snijders, *J. Chem. Phys.* **1993**, *99*, 4597.
 [26] E. van Lenthe, E. J. Baerends, J. G. Snijders, *J. Chem. Phys.* **1994**, *101*, 9783.
 [27] E. van Lenthe, A. Ehlers, E.-J. Baerends, *J. Chem. Phys.* **1999**, *110*, 8943.
 [28] S. Grimme, J. Antony, S. Ehrlich, H. Krieg, *J. Chem. Phys.* **2010**, *132*, 154104.
 [29] A. Klamt, *J. Phys. Chem.* **1995**, *99*, 2224.
 [30] A. Klamt, V. Jonas, T. Bürger, J. C. W. Lohrenz, *J. Phys. Chem. A* **1998**, *102*, 5074.

Manuscript received: June 21, 2017

Accepted manuscript online: August 4, 2017

Version of record online: September 1, 2017